

Effects of Chameleon Scalar Field on Rotation Curves of the Galaxies

Piyabut Burikham^{1,2*} and Sirachak Panpanich^{1†}

¹ *Theoretical High-Energy Physics and Cosmology Group, Department of Physics,
Faculty of Science, Chulalongkorn University, Bangkok 10330, Thailand*

² *Thailand Center of Excellence in Physics, CHE, Ministry of Education, Bangkok 10400, Thailand*

February 24, 2024

Abstract

We investigate the effects of chameleon scalar field to the effective density and pressure of a dark matter halo. The pressure is generated from the chameleonic fifth force on the matter. We demonstrate that the thick-shell non-singular boundary condition which forbids singular point leads to extremely stringent constraint on the matter-chameleon coupling when applied to galaxy. We argue that chameleon profile with central singularity is more likely to develop in general physical situation. The chameleonic fifth force from the chameleon profile with central singularity experienced by the dark matter could significantly modify the rotation curve of galaxies. The chameleonic fifth force could generate steeper cusp to the rotation curves in any dark matter profiles starting from the Navarro-Frenk-White (NFW) to the pseudo-isothermal (ISO) profile. Upper limits on the coupling constant between the chameleon and the dark matter are estimated from observational data of the late-type Low-Surface-Brightness galaxies (LSB). It is in the order of $\beta < 10^{-3}$.

Keywords: chameleon scalar field, rotation curve

*Email:piyabut@gmail.com

†Email:sirachak.p@student.chula.ac.th,sirachakp@gmail.com

1 Introduction

With series of observations in the recent years, we come to realize that the expansion of our universe is accelerating [1, 2, 3]. However, the exact cause of the acceleration is not determined for certain. The popular explanations are based on dark energy models ranging from dark energy in the form of the cosmological constant, quintessence, phantom, to the scalar-tensor, modified and $f(R)$ gravity models. The chameleon dark energy is one of the scalar-tensor theories that use scalar field to drive the accelerated expansion of the universe. This model is based on the hypothesis that a scalar field couples with matter via a conformal transformation. As a consequence, mass of the scalar field depends on the matter density in a significant way. We call this kind of scalar a chameleon scalar field after its ability to adapt itself to the environment. Its mass becomes large when the matter is abundant and becomes tiny in the low density region. Therefore it can effectively hide itself from any detection in such environment [4, 5, 6, 7]. The effects of the chameleon scalar field on the earth are consequently suppressed and the constraints on the fifth force could be evaded up to the scale of the solar system.

Since chameleon can adapt its mass very well to the environment, it can evade most gravitational constraints used to constrain other scalar gravity theories. In the models where chameleon interact with photons, the most stringent constraints on the chameleon coupling to the photon comes from Sunyaev-Zel'dovich (SZ) effect in the Cosmic Microwave Background. The SZ measurements of the Coma cluster place strong constraints on the photon-chameleon coupling. The bounds are approximately $g_{\text{eff}} < 10^{-9} - 10^{-8} \text{ GeV}^{-1}$ [8].¹ Weaker constraints come from the Earth bound experiments such as GammeV which excluded the region $2 \times 10^{-7} < g_{\text{eff}} < 4 \times 10^{-6} \text{ GeV}^{-1}$ [9].

On the other hand, the strongest constraints on the chameleonic matter coupling comes from particle colliders and it is merely $\beta < 2 \times 10^{16}$ [10, 11] (definition of β is given in Section 2). This constraint is simply the bound on the new physics mass scale typical for any new physics scenario investigated at the particle colliders ($M_{\text{new physics}} > 100 \text{ GeV}$). In contrast to the chameleon-photon coupling, no Earth-bound experiments to constrain the chameleon-matter coupling is operating. Future tests of gravity in space to measure the variation of the gravitational constant could place certain bounds on the matter-chameleon coupling [12, 13].

A useful insight regarding nature of the chameleon is the fact that even though the chameleon field increases its mass to hide its gravitational effect, the chameleon undergoes a spatial variation in doing so. When a field varies in space, it generates a density and pressure. The gradient of pressure then induces a pressure gradient force subsequently. This pressure gradient force is actually the fifth force generated by the chameleon-matter coupling [6], the very interaction responsible for changing the chameleonic mass according to the environment. In this article, we will use the effect of the chameleonic fifth force on the matter in the dark matter (DM) halo to establish an extremely stringent constraint on the chameleon-matter coupling β .

The stringent constraint on the matter-chameleon coupling from the chameleonic fifth

¹For the interaction $\mathcal{L} = -\frac{1}{4}B_F(\phi/M)F_{\mu\nu}F^{\mu\nu}$, $g_{eff} \equiv (\ln B_F)_{,\phi}(\phi_{\text{min}}/M)$.

force is a direct result of the singular chameleon solution inevitably developed in a sufficiently large massive object such as the galactic DM halo. Rapidly raising chameleon field near the singular point at the center induces appreciably large fifth force to the matter in the galaxy. The chameleonic fifth force significantly reduces the circular rotation velocity of matters in the core region. It will make the cusp of rotation curves steeper. For the late-type Low-Surface-Brightness (LSB) galaxies, the dominant gravitating element is the DM halo. We use recent observational data on the rotation curves of the LSB galaxies to place constraints on the chameleon-matter coupling. The upper bounds could be as low as $\beta < 1 \times 10^{-3}$ depending on which type of DM profile is used.

This article is organized as the following. In Section 2, we review briefly on the chameleon model and derive the equation of motion governing its profile in the presence of matter. In Section 3, we discuss the inevitability of the chameleon profile with singular point at the center of the mass distribution. Enforcing the non-singular boundary condition leads to extremely stringent constraint on the matter-chameleon coupling β (of order 10^{-7}). We argue that this boundary condition and consequently this constraint is physically unreasonable. The chameleon profile with central singularity is then numerically obtained for general situation and the density, pressure and the fifth force in the presence of a chameleon scalar field are subsequently calculated. Effects of chameleonic fifth force to the rotation curves of LSB galaxies are explored in Section 4 and 5. Constraints on the upper bound of the matter-chameleon coupling constant are obtained and discussed in Section 5. Changes of the power index in the power-law self potential of chameleon are shown not to affect most results. Section 6 concludes our work.

2 Effective Density, Pressure and the Chameleonic Fifth Force

A chameleon scalar field interacts with matter through a conformal coupling which could be absorbed into the matter action as the following [4],

$$S = \int d^4x \sqrt{-g} \left[\frac{M_{Pl}^2}{2} R - \frac{1}{2} (\partial\phi)^2 - V(\phi) \right] - \int d^4x \mathcal{L}_{matter}(\tilde{g}_{\mu\nu}, \psi_m), \quad (1)$$

where $\tilde{g}_{\mu\nu} = A^2(\phi)g_{\mu\nu}$, $A(\phi) = e^{\beta\phi/M_{Pl}}$ is a conformal coupling.

In order to find the effective density and pressure, we need to determine the profile of the chameleon in dark matter (DM) halo. We set the dynamics of the chameleon in the thick-shell regime [4, 14]. Namely, we assume that the value of scalar field which minimizes the effective potential (ϕ_{min}) only stays at the exterior of the dark matter halo. The value of the scalar field in the interior of the halo is not ϕ_{min} but $\phi(r)$ which is determined by the matter density of the halo. The equation of motion of the chameleon scalar field is [5]

$$\nabla^2\phi = V_{,\phi} + \alpha_\phi \rho_m A(\phi), \quad (2)$$

where ϕ is the chameleon scalar field, ρ_m is the matter density, and $\alpha_\phi \equiv \frac{\partial \ln A(\phi)}{\partial \phi}$. We can use available density profiles of dark matter such as the Navarro-Frenk-White (NFW) [15] and

the pseudo-isothermal (ISO) profile [16] to simulate the effects of the chameleon pressure to the DM halo.

For simplicity, we assume that the dark matter halo has spherical symmetry and the chameleon scalar field is static. The effect of spacetime curvature for the DM halo on the chameleon profile is negligible. Therefore, Eqn.(2) is reduced to

$$\frac{\partial^2 \phi}{\partial r^2} + \frac{2}{r} \frac{\partial \phi}{\partial r} = V_{,\phi} + \alpha_\phi \rho_m(r) A(\phi). \quad (3)$$

First we will consider the scalar self potential in the form of the inverse-power-law potential $V(\phi) = \frac{M^{4+n}}{\phi^n}$ [17, 18, 4, 5]. Even though this form of self potential is extremely constrained if not already ruled out by the Lunar Laser Ranging (LLR) experiment and cosmological constraints Ref. [19], it contains minimal amount of parameters and serves as the simplest chameleon model. A more viable self potential of the form $V(\phi) = M^4(1 + \mu(M/\phi)^n)$ which has not been ruled out by the same analyses, having one extra parameter μ , will be compatible with our result with the substitution $M^{4+n} \rightarrow \mu M^{4+n}$ (since only V, ϕ appears in the equation of motion). With the power-law self potential, the equation of motion becomes

$$\frac{\partial^2 \phi}{\partial r^2} + \frac{2}{r} \frac{\partial \phi}{\partial r} = -n \frac{M^{4+n}}{\phi^{n+1}} + \frac{\beta}{M_{Pl}} \rho_m(r) e^{\beta\phi/M_{Pl}}. \quad (4)$$

The right-hand side of the equation can be defined to be the derivative with respect to the chameleon field of an effective potential

$$V_{eff} = V + \rho_m(r) e^{\beta\phi/M_{Pl}}. \quad (5)$$

The value of chameleon ϕ_{min} which gives minimum effective potential is then given by

$$\phi_{min} = \left(\frac{n M^{4+n} M_{Pl}}{\rho_m \beta} \right)^{\frac{1}{n+1}}. \quad (6)$$

For our purpose, we will define ϕ_{min} for $\rho_m = \rho_\infty$ (average density of the universe) $\simeq 10^{-26}$ kg/m³.

To consider gravitational effects of the DM halo and the chameleon, we solve the Einstein equations for a spherically symmetric metric

$$ds^2 = -A(r) dt^2 + B(r) dr^2 + r^2 d\theta^2 + r^2 \sin^2 \theta d\phi^2. \quad (7)$$

The Einstein equations are

$$\frac{B-1}{Br^2} + \frac{B'}{B^2 r} = -8\pi G T_t^t, \quad (8)$$

$$\frac{B-1}{Br^2} - \frac{A'}{rAB} = -8\pi G T_r^r. \quad (9)$$

The energy-momentum tensor in the Einstein equations are the total energy-momentum tensor ($T_{(total)}^{\mu\nu} = T_{(matter)}^{\mu\nu} + T_{(\phi)}^{\mu\nu}$) due to the coupling with matter. From action of the chameleon scalar field, we obtain

$$T_{\nu}^{\mu(\phi)} = \partial^{\mu}\phi\partial_{\nu}\phi - \delta_{\nu}^{\mu}\left(\frac{1}{2}g^{\alpha\beta}\partial_{\alpha}\phi\partial_{\beta}\phi + V(\phi)\right) \quad (10)$$

and

$$T_{t(\phi)}^t = -\rho_{(\phi)} = -\frac{\phi'^2}{2B} - \frac{M^{4+n}}{\phi^n}, \quad (11)$$

$$T_{r(\phi)}^r = P_{(\phi)}^r = \frac{\phi'^2}{2B} - \frac{M^{4+n}}{\phi^n}, \quad (12)$$

$$T_{\theta(\phi)}^{\theta} = T_{\phi}^{\phi} = -\frac{\phi'^2}{2B} - \frac{M^{4+n}}{\phi^n} = P^{\theta} = P^{\phi}. \quad (13)$$

This is an isotropic distribution with curious behaviour which needs extra caution since P^r and P^{θ}, P^{ϕ} are not necessarily equivalent². Substitute into the Einstein field equations, the metric then has to satisfy

$$\frac{(B-1)}{Br^2} + \frac{B'}{B^2r} = 8\pi G\left(\rho_m(r) + \frac{\phi'^2}{2B} + \frac{M^{4+n}}{\phi^n}\right), \quad (14)$$

$$\frac{(B-1)}{Br^2} - \frac{A'}{rAB} = 8\pi G\left(-P_m - \frac{\phi'^2}{2B} + \frac{M^{4+n}}{\phi^n}\right). \quad (15)$$

In the equation of motion of the chameleon scalar field, we will set the pressure of matter to zero by assuming that the matter in the universe is in the dust form and ignoring the possible annihilation pressure of dark matter and such [20]. The effective pressure thus only comes from the scalar field. The effective density and effective pressure are then

$$\rho_{eff} = \rho_m(r) + \frac{\phi'^2}{2B} + \frac{M^{4+n}}{\phi^n}, \quad (16)$$

$$P_{eff}^r = \frac{\phi'^2}{2B} - \frac{M^{4+n}}{\phi^n} \quad (17)$$

respectively. Observe that the contribution of β comes in the determination of the chameleon profile Eqn. (4). The effective pressure from the chameleon will thus change with varying β through the changes in the chameleon profile in the dark matter halo. However, the dynamics of the matter with respect to the profile of the chameleon can be obtained directly from the conservation of the energy-momentum tensor

$$\nabla_{\mu}T_{(matter)}^{\mu\nu} + \nabla_{\mu}T_{(\phi)}^{\mu\nu} = 0, \quad (18)$$

²In terms of the pressure gradient force when reduced to the Euler equation of the chameleonic fluid, there will be extra term $\frac{1}{r}(2P^r - P^{\theta} - P^{\phi})$ in addition to $\frac{dP^r}{dr}$ in the radial direction. This term is required in order to obtain the correct fifth force expression as in Eqn. (20).

which leads to

$$\rho_m \partial_t \vec{v} = -\frac{\beta}{M_{Pl}} \rho_m \vec{\nabla} \phi, \quad (19)$$

or

$$\vec{a} = -\frac{\beta}{M_{Pl}} \vec{\nabla} \phi, \quad (20)$$

by using the equation of motion, Eqn. (4), and assuming a pressureless matter (see also the Appendix A). Namely, the chameleon-matter coupling induces the *fifth force* acting onto the matter (Ref. [6]). This fifth force could change the rotation curve of the galaxy substantially provided that the variation of the chameleon is sufficiently large as we shall see later in Section 4.

3 Constraints on the matter-chameleon coupling and singular solutions of the chameleon

In this section, we will demonstrate starting from the thick-shell regime, that the chameleon profile within a sufficiently large massive object can satisfy the non-singular boundary and positivity condition, $\phi'(0) = 0, \phi(\vec{r}) \geq 0$ only when $\beta \leq \beta_{\max}$.

For a region with sufficiently large matter density ρ_m , an excellent approximation of the chameleon profile can be obtained analytically. Since M_{pl} is large ($\simeq 2.4 \times 10^{18}$ GeV) and M is small ($\simeq 10^{-3}$ eV), we can approximate $\alpha_\phi \rho(r) A(\phi) \simeq \frac{\beta \rho(r)}{M_{pl}}$ and neglect the potential term in the equation of motion to obtain

$$\phi'(r) \simeq \frac{\beta}{4\pi M_{pl}} \left(\frac{M(r)}{r^2} \right) + \frac{1}{r^2} (\phi' r^2|_{r=0}). \quad (21)$$

For a boundary condition

$$\phi(r_{max}) = \phi_{min}, \phi'(r_{max}) \equiv \frac{\gamma \beta}{4\pi M_{pl} r_{max}^2}, \quad (22)$$

the general solution can be written as

$$\phi'(r) = \frac{\beta}{4\pi M_{pl} r^2} (M(r) - M_0 + \gamma), \quad (23)$$

where γ represents (proportional to) the slope of chameleon profile at the boundary of the mass distribution and M_0 is the total mass of the object (e.g. galaxy) at r_{max} . This expression can be integrated directly for any mass profile $M(r)$ to obtain the corresponding chameleon solution.

There are three classes of positive solutions categorized by the value of γ ,

1. $\gamma < M_0$; singular at $r = 0$

2. $\gamma = M_0$; $\phi' r^2|_{r=0} = 0$ (nonsingular)
3. $\gamma > M_0$; truncated at finite r (unphysical).

Varying the slope $\gamma > 0$, various chameleon solutions (using the full equation of motion, Eqn. (4), with the potential included) for sufficiently small β can be obtained numerically as are shown in Fig. 1. All three kinds of solutions are presented.

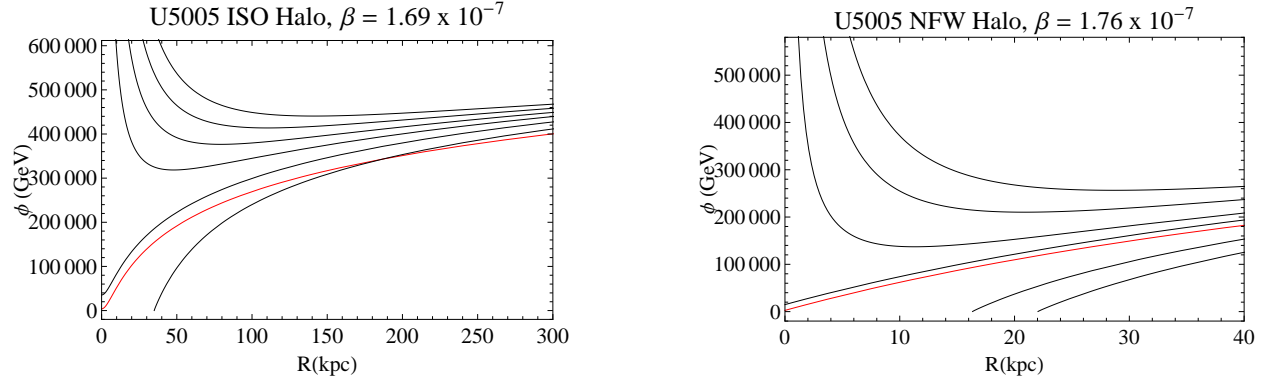


Figure 1: The chameleon solutions for various γ . The red curve is the approximated analytic solution neglecting the potential $V(\phi)$. The ISO solution (left) satisfies non-singular boundary condition $\phi'(0) = 0$ but not the NFW (right). The other curves are obtained numerically.

The third kind of solution is unphysical since it is truncated at finite radial distance. Among the remaining physical solutions, the only nonsingular one satisfies the boundary condition $\phi' r^2|_{r=0} = 0$ (class 2). The nonsingular solutions of the chameleon are investigated by most literature with the boundary condition $\phi'(0) = 0$ and finite $\phi(0)$. In the following subsection, we will demonstrate that for certain matter profiles, this boundary condition cannot be satisfied. And for those matter profiles, the most natural chameleon solution would be the singular one.

3.1 Analytic solutions for small potential and remarks on thick-shell boundary conditions

In this subsection, we consider analytic solutions of the chameleon coupling to various DM models: the NFW, ISO, and the parametrized model (PM). The potential term $V(\phi)$ will be neglected. Subsequently, both the approximated analytic and numerical (with the potential included) solutions will be compared and justified the validity of the approximation. We will investigate whether which DM profile allows non-singular chameleonic solution with flat boundary condition $\phi'(0) = 0$.

For nonsingular case in class 2, we have the gradient of the scalar given in terms of the matter density as

$$\phi' r^2 = \frac{\beta}{M_{Pl}} \int \rho(r) r^2 dr, \quad (24)$$

where $\rho(r)$ is the matter distribution.

For the NFW profile : $\rho_{NFW}(r) = \frac{\rho_0}{\frac{r}{a}(1 + \frac{r}{a})^2}$. Substitute into Eqn. (24) gives

$$\phi' r^2 = \frac{a^3 \beta \rho_0}{M_{Pl}} \left(\frac{a}{a+r} + \ln(a+r) \right) + C_1. \quad (25)$$

Taking limit $r \rightarrow 0$ and assuming $\phi' \rightarrow \infty$ slower than $1/r^2$ in this limit, the constant C_1 can be determined to be

$$C_1 = -\frac{a^3 \beta \rho_0}{M_{Pl}} (1 + \ln(a)). \quad (26)$$

Therefore

$$\begin{aligned} \phi' r^2 &= \frac{a^3 \beta \rho_0}{M_{Pl}} \left(\frac{a}{a+r} + \ln(a+r) \right) - \frac{a^3 \beta \rho_0}{M_{Pl}} (1 + \ln(a)), \\ \phi'(r) &= \frac{a^3 \beta \rho_0}{M_{Pl} r^2} \left(\ln(1 + \frac{r}{a}) - \frac{r}{a+r} \right). \end{aligned} \quad (27)$$

This is the solution of ϕ' for arbitrary initial condition, $\phi'(r=0)$. The solution of the chameleon scalar field in the NFW dark matter halo can then be obtained,

$$\phi(r) = \frac{a^3 \beta \rho_0}{M_{Pl}} \left(\frac{1}{a} - \frac{\ln(1 + \frac{r}{a})}{r} \right) + \phi(0). \quad (28)$$

Thus, we can see that at the origin of the NFW dark matter halo ($r=0$) the chameleon profile cannot be flat with

$$\phi'(0) = \frac{a \beta \rho_0}{2 M_{Pl}}. \quad (29)$$

This proves conclusively that for the chameleon coupling to the NFW DM in the thick-shell regime, the chameleon field cannot satisfy the boundary condition $\phi'(0) = 0$. Figure 2 shows both the approximated analytic and numerical (with potential included) solutions, the difference is minimal.

For the ISO profile: $\rho_{ISO}(r) = \frac{\rho_0}{1 + (\frac{r}{R_s})^2}$,

$$\phi' r^2 = \frac{\beta}{M_{Pl}} \int \rho_{ISO}(r) r^2 dr,$$

leading to

$$\phi' r^2 = \frac{\beta}{M_{Pl}} R_s^3 \rho_0 \left(\frac{r}{R_s} - \arctan\left(\frac{r}{R_s}\right) \right) + C_1. \quad (30)$$

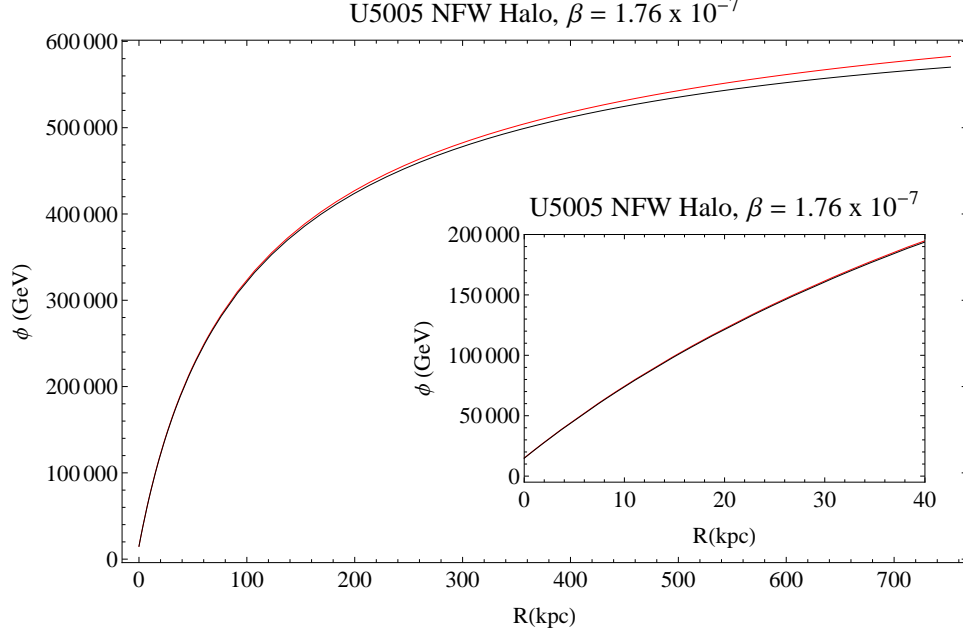


Figure 2: The chameleon profile in the NFW DM halo of U5005 galaxy for $\beta = 1.76 \times 10^{-7}$. The analytic and numerical chameleon solutions are represented in red line and black line respectively.

Taking limit $r \rightarrow 0$ and assuming $\phi' \rightarrow \infty$ slower than $1/r^2$ in this limit, we obtain $C_1 = 0$. Therefore

$$\phi'(r) = \frac{\beta R_s^3 \rho_0}{M_{Pl} r^2} \left(\frac{r}{R_s} - \arctan\left(\frac{r}{R_s}\right) \right). \quad (31)$$

Integrate to obtain solution of the chameleon scalar field in ISO dark matter halo,

$$\phi(r) = \frac{\beta R_s^3 \rho_0}{M_{Pl}} \left(\frac{\arctan(r/R_s)}{r} + \frac{\ln(1 + r^2/R_s^2)}{2R_s} - \frac{1}{R_s} \right) + \phi(0). \quad (32)$$

Thus, the chameleon profile at the origin of the ISO dark matter halo can be flat with $\phi'(0) = 0$. Figure 3 shows both the approximated analytic and numerical (potential included) solutions. The approximation becomes worse as the radial distance grows.

For the parametrized model (PM) : $\rho_{PM}(r) = \frac{\rho_0}{(\frac{r}{r_s})^\alpha (1 + \frac{r}{r_s})^{3-\alpha}}$,

$$\begin{aligned} \phi' r^2 &= \frac{\beta}{M_{Pl}} \int \rho_{PM}(r) r^2 dr, \\ &= \frac{\beta}{M_{Pl}} \frac{r^{3-\alpha} r_s^\alpha \rho_0 {}_2F_1(3-\alpha, 3-\alpha, 4-\alpha, -\frac{r}{r_s})}{3-\alpha} + C_1, \end{aligned} \quad (33)$$

where ${}_2F_1$ is the hypergeometric function.

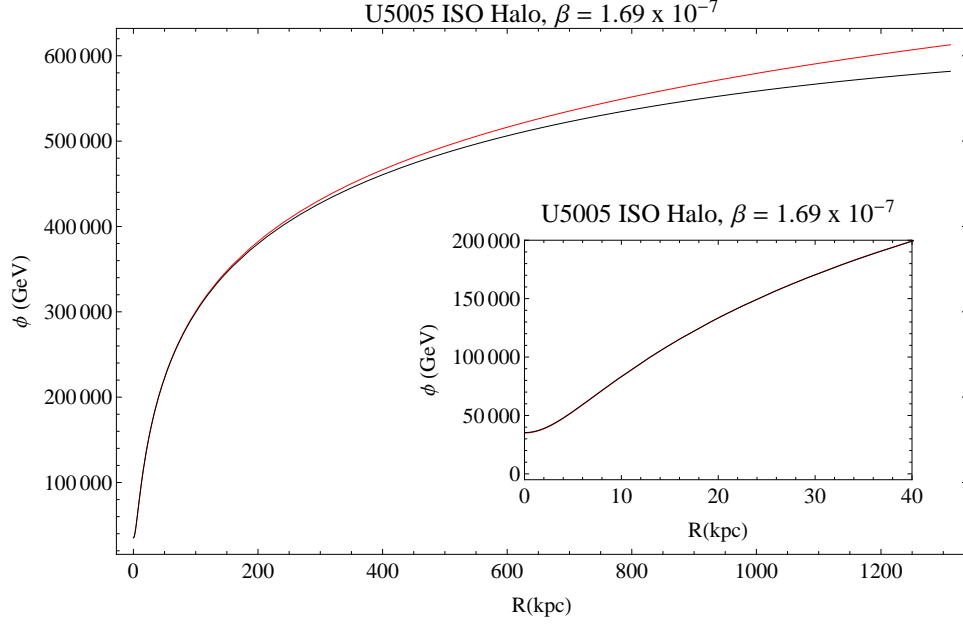


Figure 3: The chameleon profile in the ISO DM halo of U5005 galaxy for $\beta = 1.69 \times 10^{-7}$. The analytic and numerical chameleon solutions are represented in red line and black line respectively.

Taking limit $r \rightarrow 0$ and assuming $\phi' \rightarrow \infty$ slower than $1/r^2$ in this limit, we obtain $C_1 = 0$. Then

$$\phi'(r) = \frac{\beta}{M_{Pl}} \frac{r^{1-\alpha} r_s^\alpha \rho_0 {}_2F_1(3-\alpha, 3-\alpha, 4-\alpha, -\frac{r}{r_s})}{3-\alpha}, \quad (34)$$

or

$$\phi'(r) = \frac{\beta}{M_{Pl}} \frac{r^{1-\alpha} r_s^\alpha \rho_0 (1 + \frac{r}{r_s})^{\alpha-3} {}_2F_1(3-\alpha, 1, 4-\alpha, \frac{r/r_s}{1+r/r_s})}{3-\alpha}. \quad (35)$$

The value of $\phi'(0)$ for each α can then be obtained,

Case I : $\alpha < 1$

$$\phi'(0) = 0. \quad (36)$$

Case II : $\alpha = 1$ (NFW)

$$\phi'(0) = \frac{r_s \beta \rho_0}{2M_{Pl}}. \quad (37)$$

Case III : $1 < \alpha < 2$

$$\phi'(0) = \infty. \quad (38)$$

The corresponding solution of the chameleon scalar field in the PM dark matter halo is

$$\phi(r) = \frac{\beta\rho_0}{M_{Pl}} \frac{r^\alpha}{3-\alpha} \left(\frac{r^{2-\alpha}}{2-\alpha} {}_2F_1(2-\alpha, 3-\alpha, 4-\alpha, -\frac{r}{r_s}) \right) + \phi(0), \quad (39)$$

or

$$\phi(r) = \frac{\beta\rho_0}{M_{Pl}} \frac{r^\alpha}{3-\alpha} \left(\frac{r^{2-\alpha}}{2-\alpha} (1 + \frac{r}{r_s})^{\alpha-2} {}_2F_1(2-\alpha, 1, 4-\alpha, \frac{r/r_s}{1+r/r_s}) \right) + \phi(0). \quad (40)$$

where α must be less than 2. Figure 4,5,6 show both approximated analytic and numerical (potential included) solutions for the PM DM profiles, the differences are hardly visible. Figure 7 summarizes the numerical solutions for the PM model. The behaviour of the boundary value $\phi'(0)$ confirms the analytic results.

As a summary, we have shown that depending on the DM profile, the chameleon solution can NOT arbitrarily satisfy the boundary condition $\phi'(0) = 0$. The NFW and the parametrized profiles with $\alpha > 1$ (α must be less than 2 for positivity of the chameleon distribution function) cannot satisfy this flat boundary condition as shown above.

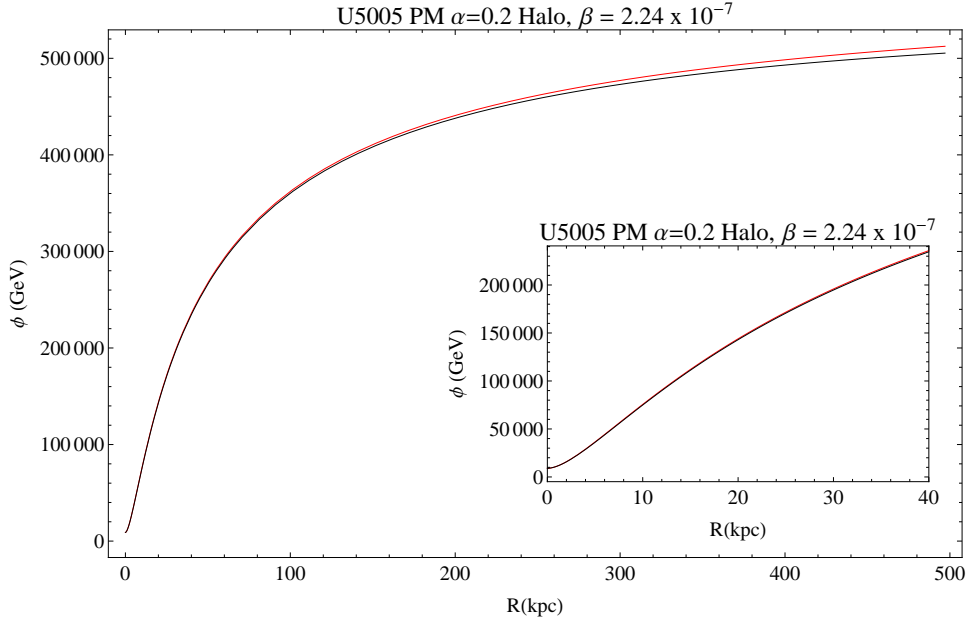


Figure 4: The chameleon profile in the PM DM halo of U5005 galaxy for $\alpha = 0.2$ and $\beta = 2.24 \times 10^{-7}$. The analytic and numerical chameleon solutions are represented in red line and black line respectively.

Now we want to derive a bound on the coupling β for the nonsingular solutions which require ϕ at the galactic edge to match ϕ_{min} of the universe. The value of ϕ_{min} is determined from the observed value of the dark energy through the self-interacting potential of the chameleon. Using the analytic formula, we can calculate the maximal matter-chameleon

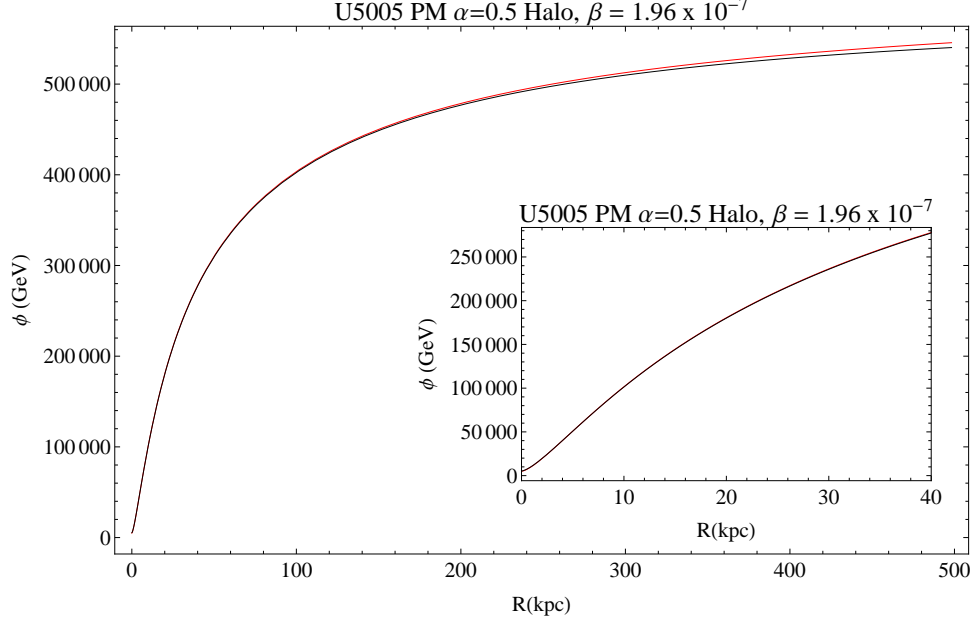


Figure 5: The chameleon profile in the PM DM halo of U5005 galaxy for $\alpha = 0.5$ and $\beta = 1.96 \times 10^{-7}$. The analytic and numerical chameleon solutions are represented in red line and black line respectively.

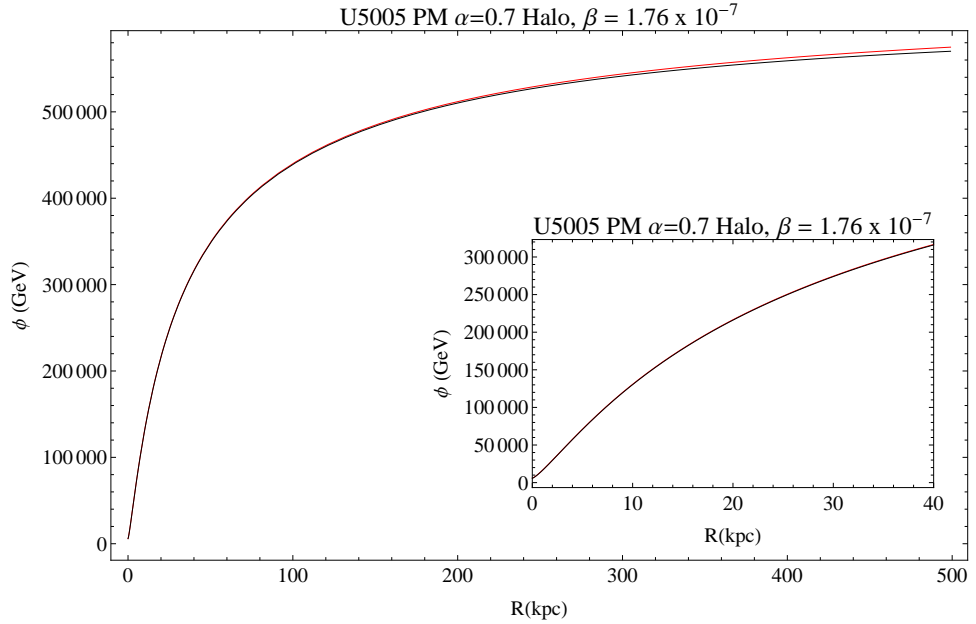


Figure 6: The chameleon profile in the PM DM halo of U5005 galaxy for $\alpha = 0.7$ and $\beta = 1.76 \times 10^{-7}$. The analytic and numerical chameleon solutions are represented in red line and black line respectively.

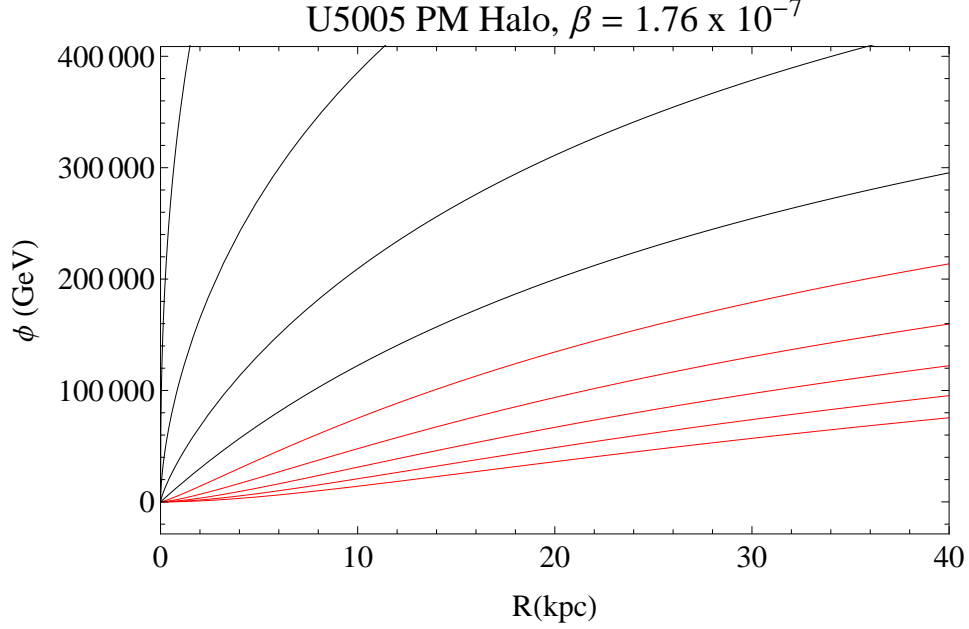


Figure 7: The analytic chameleon profiles in the PM DM halo of U5005 galaxy for $\beta = 1.76 \times 10^{-7}$. The red lines represent the chameleon profile for $0 < \alpha < 1$ and the black lines represent the chameleon profile for $1 \leq \alpha < 2$.

coupling of this solution by integrating Eqn. (21),

$$\phi_{min} \geq \frac{\beta}{4\pi M_{pl}} \int_0^{r_{max}} dr \frac{1}{r^2} M(r). \quad (41)$$

With ϕ_{min} given by Eqn. (6), the maximum β_{max} is found to be

$$\beta_{max} = \left(\frac{n M^{4+n} M_{pl}}{\rho_{\infty}} \right)^{\frac{1}{n+2}} \left[\frac{4\pi M_{pl}}{\int_0^{r_{max}} dr \frac{M(r)}{r^2}} \right]^{\frac{n+1}{n+2}}. \quad (42)$$

This crucial limit on the matter-chameleon coupling is originated from the non-singular boundary condition $\phi'(0) = 0$. As the object gets more and more massive and substantial, the maximum value of β decreases accordingly. For galaxy U5005 with ISO and NFW DM profile, the values of $\beta_{max} \simeq 1.69, 1.76 \times 10^{-7}$ respectively.

For the self potential of the form $V(\phi) = M^4(1 + \mu(M/\phi)^n)$, we can make substitution $M^{4+n} \rightarrow \mu M^{4+n}$ to obtain the limit containing two parameters β, μ as

$$\beta \lesssim \left(\frac{n\mu M^{4+n} M_{pl}}{\rho_{\infty}} \right)^{\frac{1}{n+2}} \left[\frac{4\pi M_{pl}}{\int_0^{r_{max}} dr \frac{M(r)}{r^2}} \right]^{\frac{n+1}{n+2}}. \quad (43)$$

For $n = 1$, the value of μ is constrained by the LLR experiment and cosmological conditions to be smaller than 10^5 [19], resulting in the upper limit $\beta \lesssim 10^{5/3} \beta_{max}$ for β_{max} given in

Eqn. (42). This is roughly 46 times larger than the original inverse-power-law self potential case. For NFW and ISO DM profile of galaxy U5005, the upper limit corresponds to about $\beta < 10^{-5}$.

Among the three classes of solutions mentioned earlier, only the one satisfying non-singular boundary condition was previously considered physically relevant. However, as demonstrated above, the non-singular boundary condition canNOT be satisfied for arbitrary substantially massive object such as the galactic DM halo. At the time of structure formation when the scalar field obtained their vev as the minimum of the effective potential, there is no way the chameleon could know which value the matter-chameleon coupling β should be. This value should have been fixed by some theory at the high scale. For generic situation during structure formation, the chameleon should thus develop a profile with singular point at the center $r = 0$. There is no physical reason to prevent this class of solutions for the galaxy.

3.2 Chameleon solutions with singular point

In general situation, the chameleon could develop singular profile at $r = 0$ when $\gamma < M_0$. For sufficiently large β , the chameleon solutions with $0 < \gamma < M_0$ yield mostly the same results as the case $\gamma = 0$. Without loss of generality, we will therefore consider the profile with $\gamma = 0$ and numerically solve for the profile of chameleon within the dark matter halo using the boundary condition $\phi(r_{max}) = \phi_{min}, \phi'(r_{max}) = 0$ for r_{max} defined to be the radial distance where $\rho_m(r_{max}) \simeq \rho_\infty$, the average density of the universe. We will set $n = 1$ for the chameleonic self-interacting power-law potential $V(\phi) = M^5/\phi$ and briefly discuss the negligible changes for other n in Section 5. The chameleon profiles for the NFW and ISO dark matter halo for some LSB galaxies are shown in Fig. 8.

The density of chameleon turns out to be only about 10^{-5} of the DM density and thus no distinguishable effects of the chameleon could be seen in the gravitational lensing. The gravitational contribution of the chameleon pressure is also negligible. Regardless of its smallness as a gravitational entity, the chameleon pressure gradient induces appreciable force on the DM halo in the form of the fifth force.

The chameleon changes from dark energy to matter as the density of the DM increases towards the galactic center. This is shown by the ratio $w = P_\phi/\rho_\phi$ as in Fig. 8. As it changes into some form of exotic chameleonic matter with $w = 1$, the acceleration of the test object due to the chameleonic fifth force increases as shown in Fig. 9.

4 Rotation Curves

The fifth force induced by the chameleon on the dark matter has variation along the radial direction according to Eqn. (20). The circular velocity is then reduced when the gradient of the chameleon is negative. The circular velocity which includes the acceleration due to the

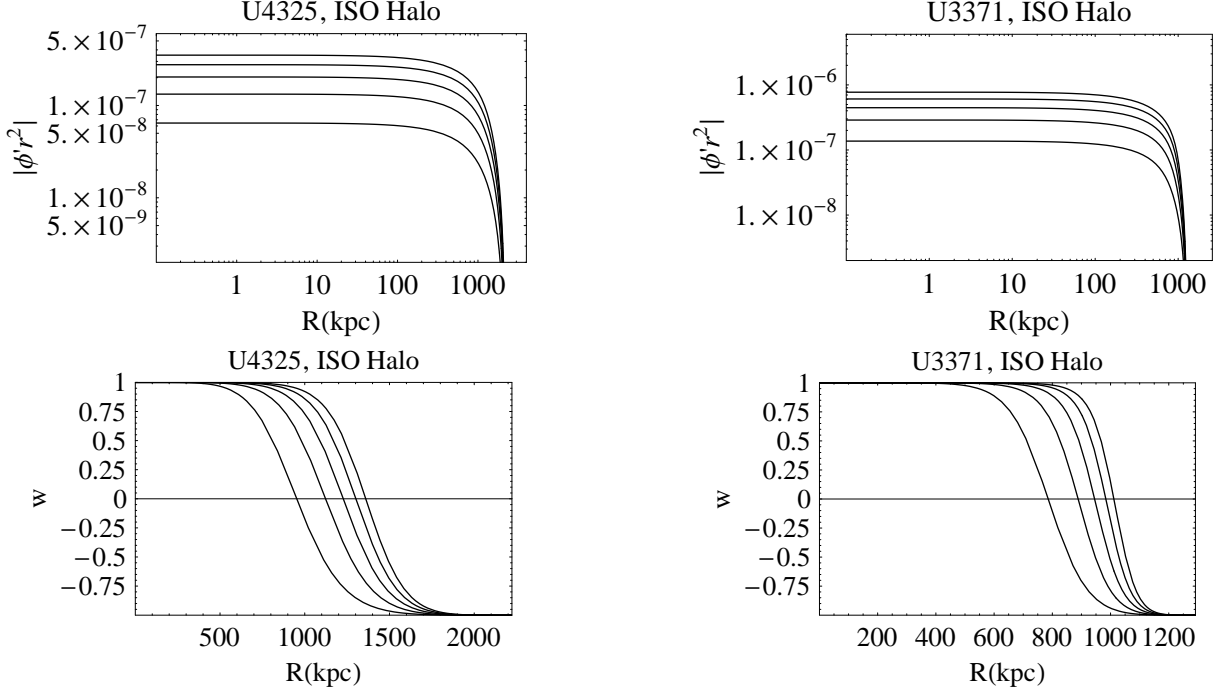


Figure 8: The chameleon profile and the ratio $w = P_\phi/\rho_\phi$ of the chameleon in the ISO DM halo of U4325, U3371 galaxy for varying $\frac{\beta}{10^{-7, -6}} = 2, 4, 6, 8, 10$ (from bottom to top graph). The chameleon field and w increase with the coupling β .

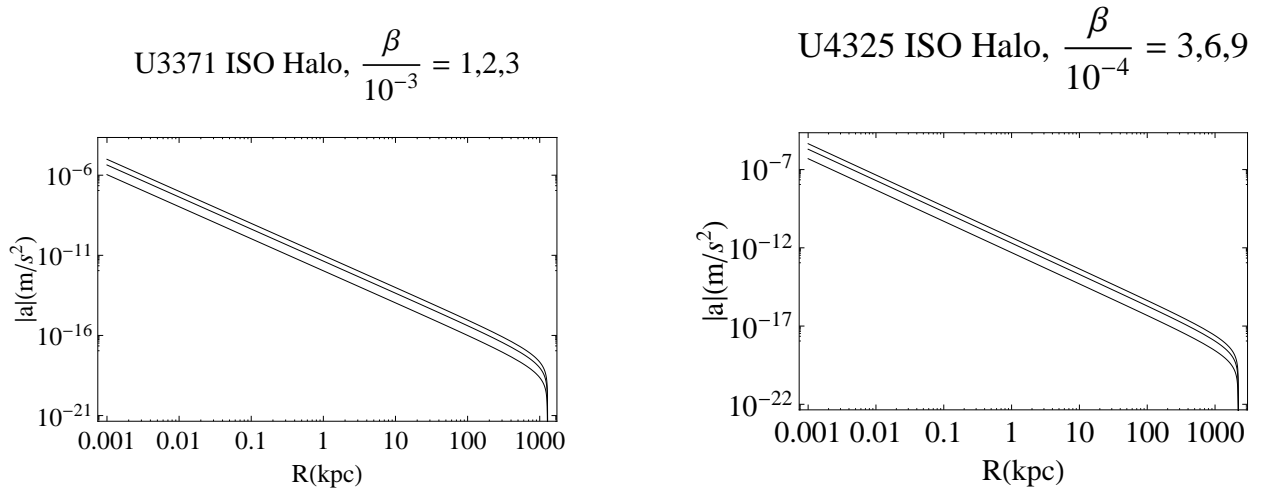


Figure 9: The acceleration from the chameleonic fifth force in the ISO DM halo of U4325, U3371 galaxy. The acceleration increases with the coupling β .

fifth force from the chameleon can be written as the following

$$v_c(r) = \sqrt{\frac{GM(r)}{r} + \frac{\beta r}{M_{Pl}} \frac{d\phi}{dr}}. \quad (44)$$

The accumulated mass of the dark matter halo depends on which mass model we are using.

The NFW DM profile emerged as the universal density profile for the dark matter halo from the simulations of Λ CDM model. The density profile depends on the critical density required to flatten the universe and therefore it is determined uniquely by the Hubble parameter H . The profile correctly gives a constant rotation velocity at large radii for most galaxies. However, recent observation of the rotation curves from the late-type LSB galaxies reveals that the center of these galaxies contains an approximately constant density core better parametrized by the ISO DM profile [21]. Among the LSB galaxies in Ref. [21], U4173, U4325, U3371, DDO185, DDO47, DDO64, U1281, DDO52, IC2233 are the galaxies which the NFW profile cannot be used to fit with the observational data of the rotation curves around the core region without stretching it to unrealistic parameters, namely too large asymptotic rotation velocity at large radii. On the other hand, the ISO profile can fit well to most LSB galaxies implying that these galaxies might actually have a constant core region.

The contrast between simulation results from the Λ CDM model and observational data is known as the core-cusp problem (see Ref. [22] for an excellent review). While the Λ CDM model supports a cuspy rotation curve, observational data of the late-type LSB galaxies prefer the mass model with a constant core. To explore the effects of the chameleonic fifth force on each kind of DM halo, we consider two popular mass models, NFW and ISO, and finally in a parametrized (PM) model.

4.1 NFW halo

For the NFW profile, the DM density is given by

$$\rho_{\text{NFW}}(r) = \frac{\rho_0}{\frac{r}{a} \left(1 + \frac{r}{a}\right)^2}, \quad (45)$$

where ρ_0 and a are the characteristic density and the scale radius of the halo respectively. Although we will use the NFW profile and effective acceleration from the chameleonic fifth force to calculate the circular velocity, we must know the characteristic density of the NFW profile. In order to obtain the ρ_0 of NFW profile, we consider the accumulated mass

$$M_{\text{NFW}}(r) = V_{200}^2 \left(\frac{\ln(1 + (cr/r_{200})) - (cr/r_{200})/(1 + (cr/r_{200}))}{\ln(1 + c) - c/(1 + c)} \right) \frac{r_{200}}{G}, \quad (46)$$

leading to the circular velocity in the absence of the chameleon as

$$v_c(r) = V_{200} \sqrt{\frac{1}{x} \frac{\ln(1 + cx) - cx/(1 + cx)}{\ln(1 + c) - c/(1 + c)}}, \quad (47)$$

where V_{200} is the circular velocity at virial radius (r_{200}), $x = r/r_{200}$ is the radial distance in unit of the virial radius and $c = r_{200}/a$ is the concentration parameter.

The characteristic density of the NFW profile is then given by

$$\rho_0 = \frac{V_{200}^2}{4\pi G a^2} \left(\frac{c}{\ln(1+c) - c/(1+c)} \right). \quad (48)$$

And from the virial mass (m_{200}), we obtain the virial radius and the characteristic radius respectively:

$$r_{200} = \frac{V_{200}}{10H}, \quad (49)$$

$$a = \frac{r_{200}}{c} \quad (50)$$

where H is the Hubble parameter.

For the late-type low surface brightness (LSB) galaxies, dominating gravitational element is the dark matter halo. It is thus the most efficient to study effects of chameleonic fifth force on the rotation curves of the LSB galaxies. Using values of V_{200} , c from Ref. [21] and $H = 72$ km/s/Mpc, we can produce the rotation curves for certain LSB galaxies shown in Fig. 10.

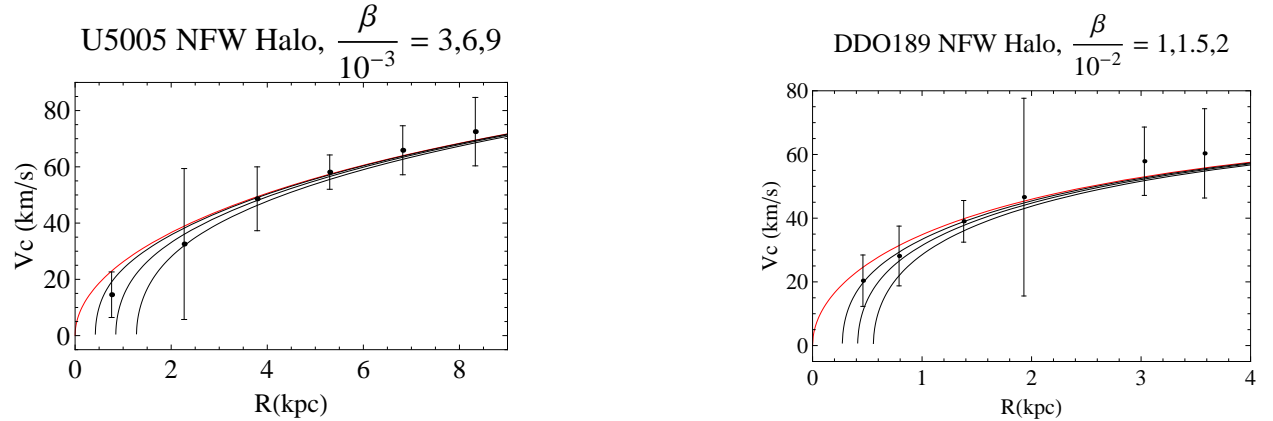


Figure 10: Rotation curves of U5005, DDO189 galaxy around the core region for varying β . The red lines represent the rotation curve of the galaxy with NFW profile without the chameleon.

4.2 ISO Halo

For a spherical pseudo-isothermal halo, the DM density profile is assumed to be

$$\rho_{\text{ISO}}(r) = \frac{\rho_c}{1 + \left(\frac{r}{R_c}\right)^2}, \quad (51)$$

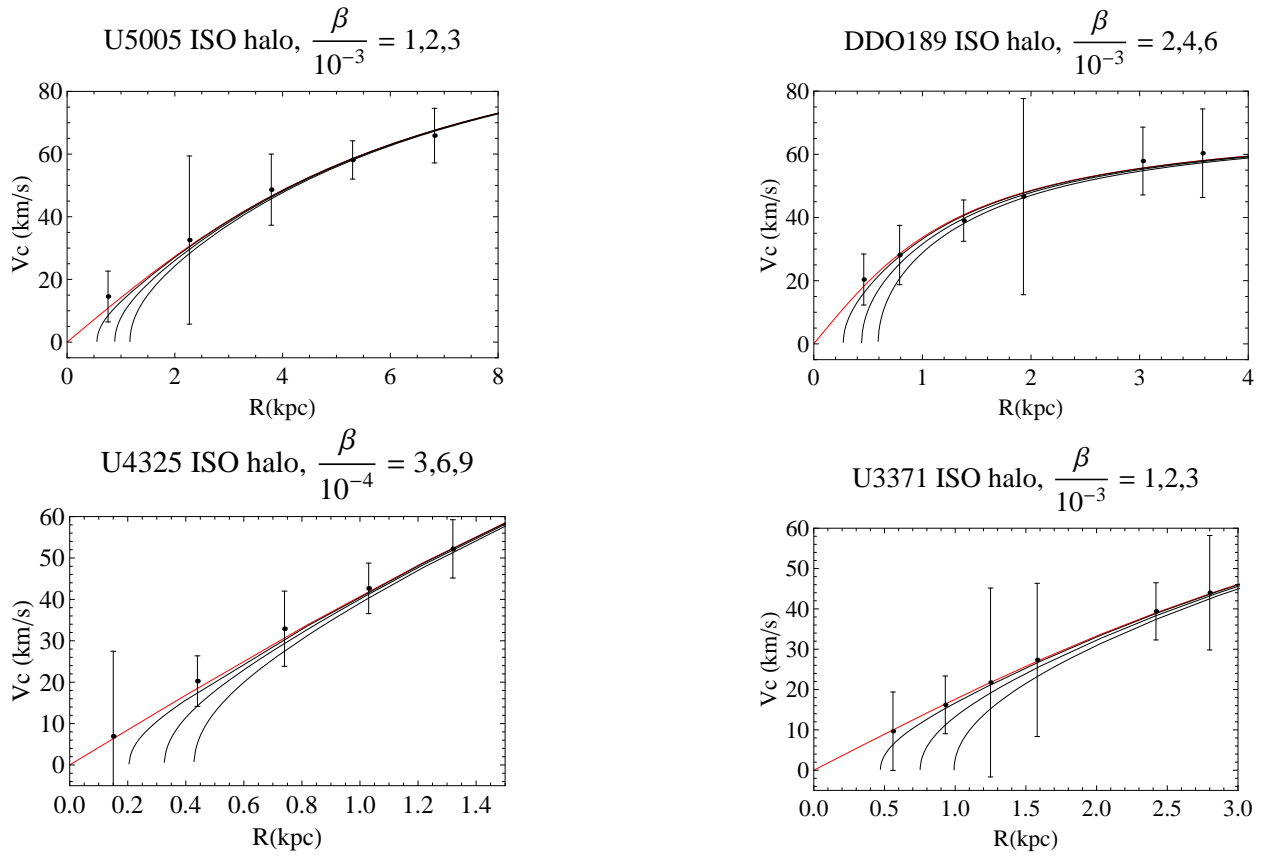


Figure 11: Rotation curves of U5005, DDO189, U4325, U3371 galaxy in the core region for varying β . The red lines represent rotation curves of the galaxy with ISO profile without the chameleon.

where ρ_c and R_c are the central density and core radius of the halo respectively. The rotation curve from this density profile in the absence of the chameleon is

$$v_c(r) = \sqrt{4\pi G \rho_c R_c^2 \left(1 - \frac{R_c}{r} \arctan\left(\frac{r}{R_c}\right)\right)}. \quad (52)$$

The best-fit parameters ρ_c, R_c and processed rotation curves of some LSB galaxies are given in Ref. [21]. We use these parameters to generate rotation curves with varying chameleon-matter coupling β as are shown in Fig. 11.

4.3 The parametrized model

We can generalize the density profile of the NFW model to be

$$\rho_{\text{PM}}(r) = \frac{\rho_0}{\left(\frac{r}{r_s}\right)^\alpha \left(1 + \frac{r}{r_s}\right)^{3-\alpha}}, \quad (53)$$

where α is a parameter which takes value of 1 for the NFW profile. This profile correctly reproduces $\rho \propto r^{-3}$ in the large radius limit. The circular rotation velocity in the absence of chameleon is then

$$v_c(r) = \sqrt{\frac{4\pi G \rho_0}{3-\alpha} r^2 \left(\frac{r}{r_s}\right)^{-\alpha} {}_2F_1(3-\alpha, 3-\alpha, 4-\alpha, -r/r_s)} \quad (54)$$

where ${}_2F_1$ is the hypergeometric function. Rotation curves of U5005, DDO189 with $\alpha = 0.2, 0.7$ and U4325, U3371 with $\alpha = 0.2$ for varying β are shown in Fig. 12.

4.4 Analytic approximation of the rotation curve

An excellent approximation of the rotation curve can be obtained analytically according to Eqn. (23). Demanding that $\phi'(r_{\text{max}}) = 0$ (*i.e.* $\gamma = 0$) at the galactic boundary, we obtain $(\phi' r^2|_{r=0}) = -\frac{\beta}{4\pi M_{\text{Pl}}} M(r_{\text{max}})$. The analytic approximation of the acceleration from the fifth force is then given by

$$a = \frac{\beta}{M_{\text{Pl}}} \phi'(r) \simeq -\frac{1}{4\pi r^2 B(r)} \left(\frac{\beta}{M_{\text{Pl}}}\right)^2 (M_0 - M(r)). \quad (55)$$

The galactic mass M_0 is again defined to be $M(r_{\text{max}})$. The force pushes outwardly when the chameleon gradient is negative. It effectively reduces the rotation velocity of matter in the galaxy. For a generic DM halo which is far from undergoing a gravitational collapse, $B(r) \simeq 1$. The acceleration from the fifth force is thus determined mostly by the mass profile and it is proportional to β^2 . Substituting into Eqn. (44), the resulting rotation curves agree extremely well with the numerical results.

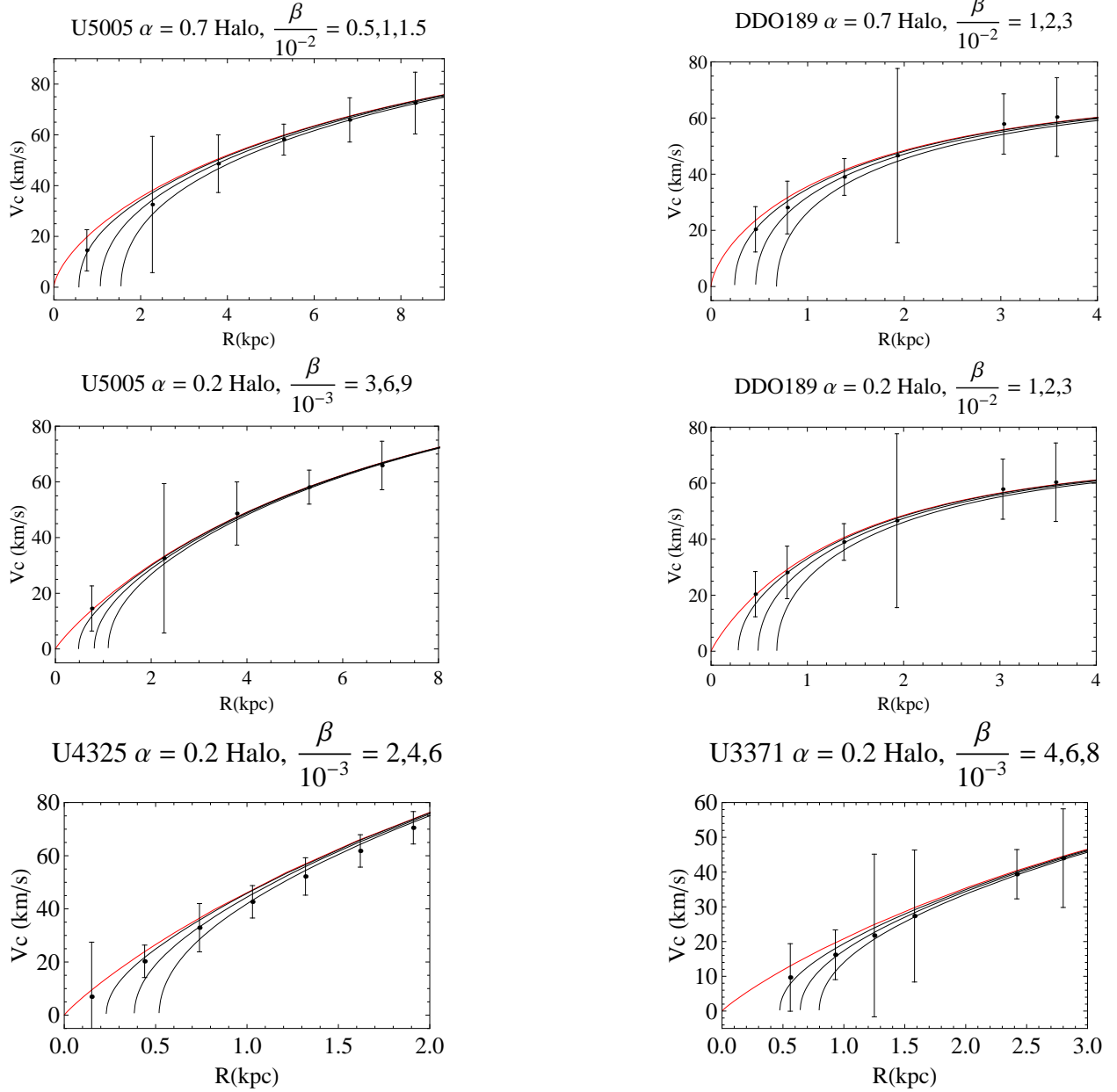


Figure 12: Rotation curves of U5005, DDO189, U4325, U3371 galaxy around the core region for varying β . U4325 and U3371 cannot be fit to the PM model with $\alpha = 0.7$ without making the rotation velocity unrealistically large. The red lines represent the rotation curves of the galaxy with the PM profile without the chameleon.

5 Results and Discussions

For NFW profile, we choose to explore the effects of chameleon in U5005 and DDO189 galaxy since the data can be fit without assuming too large circular rotation velocities. As we can see from Fig. 10, the chameleonic fifth force is larger in the core region. The rotation velocity is reduced as the fifth force drives the matter in the outward direction. For U5005, turning the value of $\beta > 6 \times 10^{-3}$ gives the rotation curve cuspiest, so much that it misses the error bar of the innermost data point. For DDO189, $\beta > 1.75 \times 10^{-2}$ results in the bad fit of the innermost data point. For statistical analysis, we use U5005 with the number of degree of freedom $N = 11 - 3 = 8$ and establish a constraint on the upper bound of matter coupling $\beta < 1 \times 10^{-3}$ at 95 % C.L. DDO189 gives less stringent constraint.

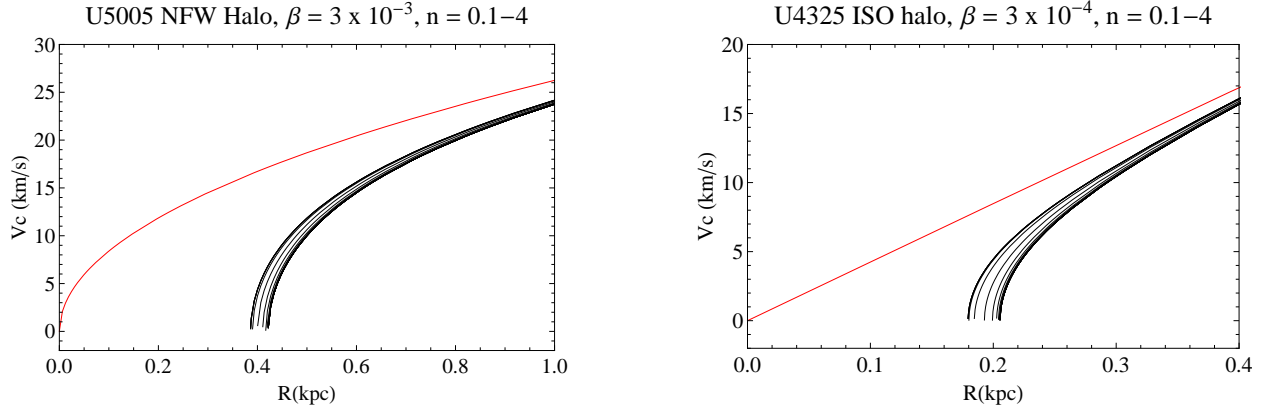


Figure 13: Rotation curves of galaxy U5005, U4325 for the chameleonic self potential $V(\phi) = M^{n+1}/\phi^n$ with $n = 0.1 - 4$ (left to right) using NFW, ISO profile. The red lines are the rotation curves without the chameleon.

For ISO profile, we present rotation curves for U5005, U4325, U3371, DDO189 galaxies with varying β . The strongest constraint on the coupling β is from U4325 where $\beta > 3 \times 10^{-4}$ results in a large deviation of the rotation curve from the innermost data point. This is shown in Fig. 11. For statistical analysis, we use U4325 with the number of degree of freedom $N = 16 - 3 = 13$ and establish a constraint on the upper bound of matter coupling $\beta < 1 \times 10^{-3}$ at 95 % C.L. Other galaxies give less stringent constraints.

The PM mass model can fit with the rotation curve data better than the NFW in the core region for $\alpha < 1$ since the cusp is less steep. For $\alpha > 1$, the quality of fit is worse, therefore we consider the PM mass model only in $\alpha < 1$ cases. This is shown in Fig. 12. Again, the chameleonic fifth force makes the cusp steeper, resulting in the worse fitting. For U5005, DDO189, large deviations of the rotation curve from the innermost data point occur when $\beta > 1, 2 \times 10^{-2}$ for $\alpha = 0.7$ respectively. For statistical analysis, we use U4325 with the number of degree of freedom $N = 16 - 3 = 13$ and establish a constraint on the upper bound of matter coupling $\beta < 5.4 \times 10^{-3}$ at 95 % C.L. for $\alpha = 0.2$. For $\alpha = 0.7$, U5005 is used with $N = 11 - 3 = 8$, the upper bound on the matter coupling becomes $\beta < 9 \times 10^{-3}$. The strongest constraints for each DM halo are summarized in Table 1. Numerical studies

LSB galaxy	upper bound on β at 95 % C.L.
U5005 (NFW)	6×10^{-3}
U5005 (ISO)	2×10^{-3}
U5005 (PM $\alpha = 0.2$)	6×10^{-3}
U5005 (PM $\alpha = 0.7$)	9×10^{-3}
DDO189 (NFW)	1.75×10^{-2}
DDO189 (ISO)	4.8×10^{-3}
DDO189 (PM $\alpha = 0.2$)	1.75×10^{-2}
DDO189 (PM $\alpha = 0.7$)	1.85×10^{-2}
U4325 (ISO)	1×10^{-3}
U4325 (PM $\alpha = 0.2$)	5.4×10^{-3}
U3371 (ISO)	2.7×10^{-3}
U3371 (PM $\alpha = 0.2$)	9.5×10^{-3}

Table 1: Constraints on the matter-chameleon coupling constant from the LSB galaxies.

show that the rotation curves change very slightly (cuspiest for larger n) for the self potential with $n = 0.1 - 4$ as shown in Fig. 13. The constraints are thus mostly the same for the power-law potential with $n = 0.1 - 4$ (only fractionally stronger).

Observe that the rotation curves are made *cuspiest* for every galaxy in the presence of the chameleon, regardless of the mass model of the DM halo. The parameters of each mass model need to be fit to the rotation curve in the large radii region and they will be the same as the best fit in the absence of the chameleon. Deviation of the rotation curves in the presence of the chameleon will appear in the core region where the effect of the chameleonic fifth force is the most distinctive.

6 Conclusions

Generically, a chameleon scalar field is designed to interact with matter through a conformal coupling so that its mass varies with the matter density locally. The chameleon becomes massive when the local density is high and the modification of gravity from the modified Yukawa potential is thus negligible. The chameleon mechanism makes the scalar field evade the constraints on the violation of Equivalence Principle and the fifth force from the Earth bound experiments.

In the situation where matter density varies, the chameleon obtains a profile with spatial variation, generating a pressure profile within the matter. The pressure gradient force is actually the fifth force induced by the chameleon-matter coupling. We demonstrate that for a sufficiently large massive object such as a galaxy, the non-singular boundary condition leads to stringent but yet unphysical constraint on the matter-chameleon coupling (roughly of order $\beta < 10^{-7}$). We argue that the physical chameleon profile in general inevitably

develop a singularity at the center. The chameleon profile with central singularity leads to a significantly large chameleonic fifth force close to the center region. In a presence of the galactic DM halo, the fifth force becomes appreciably large so that in the core region of the galaxy, the force significantly reduces the circular rotation velocity of the galaxy, resulting in a cusper rotation curve.

We investigate the effects of the chameleonic fifth force on the rotation curves of certain late-type LSB galaxies using the NFW, ISO, and parametrized mass profiles. Constraints on the upper bound at 95 % C.L. on the chameleon-matter coupling are established in Table 1. The constraints could be as stringent as $\beta < 1 \times 10^{-3}$ for the ISO mass model. For a parametrized mass model with $\alpha = 0.7, 0.2$, the constraints are not as strong, $\beta < 5-9 \times 10^{-3}$.

Analytic approximation of the rotation curve in the presence of the chameleon is derived with great accuracy. The chameleonic fifth force is determined mostly by the mass profile of the DM halo and it is proportional to the matter coupling β^2 . The force is directed outward since the chameleon gradient is negative. The force is strongest in the core region and the rotation curve is altered the most in the region. The chameleon therefore generates cusper rotation curves for every mass model of the DM halo.

Acknowledgments

We would like to thank Maneenate Wechakama and Wiphu Rujopakarn for valuable discussions and suggestion on the LSB galaxy data. P.B. and S.P. are supported in part by the 90th Year Chulalongkorn Scholarship and Toray Science Foundation, Japan (TSF). P.B. is supported in part by Thailand Center of Excellence in Physics (ThEP).

A Derivation of the chameleonic fifth force

From the chameleon-matter action

$$S = \int d^4x \sqrt{-g} \left(\frac{M_{Pl}^2}{2} R - \frac{(\partial\phi)^2}{2} - V(\phi) \right) - \int d^4x \mathcal{L}_m(\psi_m, A^2(\phi) g_{\mu\nu}),$$

after varying with respect to the field, ϕ , we obtain an equation of motion of the chameleon as

$$\nabla^2 \phi = V_{,\phi} - \alpha_\phi T_\mu^{\mu(m)}. \quad (56)$$

The above equation must be consistent with the equation from $\nabla^\mu T_{\mu\nu} = 0$. Since the chameleon scalar field couple with matter, then

$$\nabla^\mu T_{\mu\nu}^{(total)} = \nabla^\mu T_{\mu\nu}^{(m)} + \nabla^\mu T_{\mu\nu}^{(\phi)} = 0. \quad (57)$$

The energy-momentum tensor of the scalar field is

$$T_{\mu\nu}^{(\phi)} = \partial_\mu \phi \partial_\nu \phi - g_{\mu\nu} \left(\frac{1}{2} g^{\alpha\beta} \partial_\alpha \phi \partial_\beta \phi + V(\phi) \right).$$

Thus

$$\begin{aligned}
\nabla^\mu T_{\mu\nu}^{(\phi)} &= (\nabla^\mu \partial_\mu \phi) \partial_\nu \phi + \partial_\mu \phi (\nabla^\mu \partial_\nu \phi) - g_{\mu\nu} \nabla^\mu \left(\frac{1}{2} g^{\alpha\beta} \partial_\alpha \phi \partial_\beta \phi + V(\phi) \right), \\
&= (\nabla^\mu \nabla_\mu \phi) \partial_\nu \phi + \partial_\mu \phi (\nabla^\mu \partial_\nu \phi) - g_{\mu\nu} (\nabla^\mu (\frac{1}{2} \partial_\alpha \phi \partial^\alpha \phi) + \nabla^\mu V(\phi)), \\
&= (\nabla^2 \phi) \partial_\nu \phi + \partial_\mu \phi (\nabla^\mu \partial_\nu \phi) - \partial^\alpha \phi \nabla_\nu \partial_\alpha \phi - V_{,\phi} \partial_\nu \phi, \\
&= (\nabla^2 \phi - V_{,\phi}) \partial_\nu \phi + \partial_\mu \phi (\nabla^\mu \partial_\nu \phi) - \partial^\alpha \phi \nabla_\nu \partial_\alpha \phi,
\end{aligned}$$

where

$$\begin{aligned}
\nabla_\nu \partial_\alpha \phi &= \partial_\nu \partial_\alpha \phi - \Gamma_{\nu\alpha}^\lambda \partial_\lambda \phi, \\
\nabla^\mu \partial_\nu \phi &= g^{\mu\alpha} \partial_\alpha \partial_\nu \phi - g^{\mu\alpha} \Gamma_{\alpha\nu}^\lambda \partial_\lambda \phi, \\
&= \partial^\mu \partial_\nu \phi - g^{\mu\alpha} \Gamma_{\alpha\nu}^\lambda \partial_\lambda \phi.
\end{aligned}$$

Then

$$\begin{aligned}
\partial_\mu \phi (\nabla^\mu \partial_\nu \phi) - \partial^\alpha \phi \nabla_\nu \partial_\alpha \phi &= \partial_\mu \phi (\partial^\mu \partial_\nu \phi - g^{\mu\alpha} \Gamma_{\alpha\nu}^\lambda \partial_\lambda \phi) - \partial^\alpha \phi (\partial_\nu \partial_\alpha \phi - \Gamma_{\nu\alpha}^\lambda \partial_\lambda \phi), \\
&= -\partial^\alpha \phi \Gamma_{\alpha\nu}^\lambda \partial_\lambda \phi + \partial^\alpha \phi \Gamma_{\nu\alpha}^\lambda \partial_\lambda \phi, \\
&= 0.
\end{aligned}$$

Therefore

$$\nabla^\mu T_{\mu\nu}^{(\phi)} = (\nabla^2 \phi - V_{,\phi}) \partial_\nu \phi.$$

From the equation of motion of the chameleon (Eqn. (56)), we obtain

$$\begin{aligned}
\nabla^\mu T_{\mu\nu}^{(\phi)} &= -\alpha_\phi T \partial_\nu \phi, \\
&= \alpha_\phi \rho \partial_\nu \phi.
\end{aligned}$$

From Eqn. (57), the covariant derivative of the matter is then

$$\nabla^\mu T_{\mu\nu}^{(m)} = -\alpha_\phi \rho \partial_\nu \phi.$$

For non-relativistic fluid and approximately flat spacetime, the LHS becomes

$$\rho(\partial_t v^i + \vec{v} \cdot \vec{\nabla} v^i) + \partial_i P = -\alpha_\phi \rho \partial_i \phi.$$

We approximate the matter to be pressureless while the gradient has only the radial direction due to spherical symmetry ($\vec{v} \cdot \vec{\nabla} = 0$). Therefore

$$\rho(\partial_t v^i) = -\alpha_\phi \rho \partial_i \phi,$$

then

$$\vec{a} = -\alpha_\phi \vec{\nabla} \phi.$$

This is the acceleration due to the fifth force from the chameleon acting on the matter. Therefore, if we consider only the effects on the matter in presence of gravity, we will obtain the circular velocity of matter within the galaxy as

$$v_c(r) = \sqrt{\frac{GM(r)}{r} + \alpha_\phi (\partial_r \phi) r}.$$

References

- [1] R. A. Knop *et al.* [Supernova Cosmology Project Collaboration], *Astrophys. J.* **598** (2003) 102 [arXiv:astro-ph/0309368].
- [2] J. C. Mather, D. J. Fixsen, R. A. Shafer, C. Mosier and D. T. Wilkinson, *Astrophys. J.* **512** (1999) 511 [arXiv:astro-ph/9810373].
- [3] E. Komatsu *et al.*, [arXiv:1001.4538, astro-ph.CO].
- [4] J. Khoury and A. Weltman, *Phys. Rev.* **D69**, 044026 (2004) [arXiv:astro-ph/0309411].
- [5] P. Brax, C. van de Bruck, A. C. Davis, J. Khoury and A. Weltman, *AIP Conf. Proc.* **736**, 105 (2005) [arXiv:astro-ph/0410103].
- [6] Ph. Brax, C. van de Bruck and A. C. Davis, *JCAP* **0411**, 004 (2004) [arXiv:astro-ph/0408464].
- [7] T. P. Waterhouse, [arXiv:astro-ph/0611816].
- [8] A. C. Davis, C. A. O. Schelpe, and D. J. Shaw, *Phys. Rev.* **D80**, 064016 (2009) [arXiv:0907.2672v2, astro-ph.CO].
- [9] A.S. Chou, W. Wester, A. Baumbaugh, H.R. Gustafson, Y. Irizarry-Valle, P.O. Mazur, J.H. Steffen, R. Tomlin, A. Upadhye, A. Weltman, X. Yang, J. Yoo, *Phys. Rev. Lett.* **102**, 030402 (2009) [arXiv:0806.2438v2, hep-ex].
- [10] David F. Mota and Douglas J. Shaw, *Phys. Rev.* **D75**, 063501 (2007) [arXiv:hep-ph/0608078].
- [11] David F. Mota and Douglas J. Shaw, *Phys. Rev. Lett.* **97**, 151102 (2006) [arXiv:hep-ph/0606204].
- [12] J. Khoury and A. Weltman, *Phys. Rev. Lett.* **93** (2004) 171104 [arXiv:astro-ph/0309300].
- [13] P. Brax, C. van de Bruck, A. C. Davis, J. Khoury and A. Weltman, *Phys. Rev.* **D70** (2004) 123518 [arXiv:astro-ph/0408415].
- [14] T. Tamaki and S. Tsujikawa, *Phys. Rev.* **D78**, 084028 (2008) [arXiv:0808.2284 [gr-qc]].
- [15] J. F. Navarro, C. S. Frenk and S. D. M. White, *Astrophys. J.* **462**, 563 (1996) [arXiv:astro-ph/9508025].
- [16] K. G. Begeman, A. H. Broeils and R. H. Sanders, *Mon. Not. Roy. Astron. Soc.* **249** (1991) 523.
- [17] I. Zlatev, L. Wang, P. J. Steinhardt, *Phys. Rev. Lett.* **82**, (1999) 896 [arXiv:astro-ph/9807002].

- [18] P. J. Steinhardt, L. Wang, I. Zlatev, Phys. Rev. **D 59** (1999) 123504 [arXiv:astro-ph/9812313].
- [19] R. Gannouji, B. Moraes, D. F. Mota, D. Polarski, S. Tsujikawa, H. A. Winther, Phys. Rev. **D 82** (2010) 124006 [arXiv:1010.3769, astro-ph.CO].
- [20] M. Wechakama and Y. Ascasibar, Mon. Not. Roy. Astron. Soc. **413** (2011) 1991 [arXiv:1007.3179, astro-ph.CO].
- [21] W. J. G. de Blok and A. Bosma, Astron. Astrophys. **385** (2002) 816 [arXiv:astro-ph/0201276].
- [22] W. J. G. de Blok, [arXiv:astro-ph/0910.3538].